Article

Polymer Microchips Integrating Solid-Phase Extraction and High-Performance Liquid Chromatography Using Reversed-Phase Polymethacrylate Monoliths

Jikun Liu, Chien-Fu Chen, Chia-Wen Tsao, Chien-Cheng Chang, Chin-Chou Chu, and Don L. DeVoe

Anal. Chem., **2009**, 81 (7), 2545-2554• DOI: 10.1021/ac802359e • Publication Date (Web): 06 March 2009

Anal. Chem. **2009,** *81,* 2545–2554

Polymer Microchips Integrating Solid-Phase Extraction and High-Performance Liquid Chromatography Using Reversed-Phase Polymethacrylate Monoliths

Jikun Liu,[†] Chien-Fu Chen,[†,‡] Chia-Wen Tsao,[†] Chien-Cheng Chang,[‡] Chin-Chou Chu,[‡] and Don L. DeVoe*[,†]

Department of Mechanical Engineering, University of Maryland, College Park, Maryland, and Institute of Applied Mechanics, National Taiwan University, Taipei, Taiwan

Polymer microfluidic chips employing in situ photopolymerized polymethacrylate monoliths for high-performance liquid chromatography separations of peptides is described. The integrated chip design employs a 15 cm long separation column containing a reversed-phase polymethacrylate monolith as a stationary phase, with its front end seamlessly coupled to a 5 mm long methacrylate monolith which functions as a solid-phase extraction (SPE) element for sample cleanup and enrichment, serving to increase both detection sensitivity and separation performance. In addition to sample concentration and separation, solvent splitting is also performed on-chip, allowing the use of a conventional LC pump for the generation of on-chip nanoflow solvent gradients. The integrated platform takes advantage of solvent bonding and a novel high-pressure needle interface which together enable the polymer chips to withstand internal pressures above 20 MPa (~2900 psi) for efficient pressure-driven HPLC separations. Gradient reversed-phase separation of fluorescein-labeled model peptides and BSA tryptic digest are demonstrated using the microchip HPLC system. Online removal of free fluorescein and enrichment of labeled proteins are simultaneously achieved using the on-chip SPE column, resulting in a 150-fold improvement in sensitivity and a 10-fold reduction in peak width in the following microchip gradient LC separation.

Since the debut of microchip capillary electrophoresis (CE) in 1992,[1] the development of microfluidic separation techniques has been a major focus of laboratory-on-a-chip research efforts. While significant advances in the development of electrokinetic separations in microfluidic platforms have been reported, research toward the miniaturization of pressure-driven high-performance liquid chromatography (HPLC) systems has not received the same level of attention.[2] A highly reliable and versatile separation technique, HPLC based on silica capillary columns plays a central role in a host of modern bioanalytical methods, such as the combination of strong cation exchange (SCX) and reversed-phase (RP) LC for application to multidimensional protein identification technology (MudPIT) analysis.[3] In comparison to electrokinetic separations, flow rates in HPLC are insensitive to variations in microchannel surface properties along the separation path, a crucial benefit toward the reproducible analysis of biological samples. Sample consumption in microfluidic HPLC can be significantly reduced using well-designed sample injectors. Microfabrication can offer a number of other benefits, particularly by providing higher levels of integration and simplifying instrumentation demands for HPLC analysis. A further critical benefit of microfludic technology for HPLC is that multiple separation elements can be fabricated in a single device to perform high-throughput parallel analysis.

Following the introduction of microfabricated silicon LC chips by Manz and co-workers in 1990,[4,5] research on microfabricated pressure-driven HPLC remained scarce until 2000, when Erickson et al. demonstrated rapid anion-exchange LC separation of four model proteins within 1 min using a quartz HPLC microchip.[6] Seki and colleagues later separated bovine serum albumin (BSA) and immunoglobulin G (IgG) by anion-exchange chromatography using a polydimethylsiloxane (PDMS) microchip,[7] while Vahey et al. fabricated a PDMS pressure-driven open tubular liquid chromatography (OTLC) microchip to analyze salt, indicator, and dyes,[8] and Schlund et al. reported an OTLC microchip driven by

* To whom correspondence should be addressed. Prof. Don L. DeVoe, Department of Mechanical Engineering, 3125 Martin Hall, University of Maryland, College Park, MD 20742. E-mail: ddev@eng.umd.edu. Fax: +1-301-314-9477.

[†] University of Maryland.

[‡] National Taiwan University.

(1) Manz, A.; Harrison, D. J.; Verpoorte, E. M. J.; Fettinger, J. C.; Paulus, A.; Ludi, H.; Widmer, H. M. *J. Chromatogr.* **1992**, *593*, 253–258.

(2) de Mello, A. *Lab Chip* **2002**, *2*, 48N–54N.

(3) Link, A. J.; Eng, J.; Schieltz, D. M.; Carmack, E.; Mize, G. J.; Morris, D. R.; Garvik, B. M.; Yates, J. R. *Nat. Biotechnol.* **1999**, *17*, 676–682.

(4) Manz, A.; Miyahara, Y.; Miura, J.; Watanabe, Y.; Miyagi, H.; Sato, K. *Sens. Actuators, B: Chem.* **1990**, *1*, 249–255.

(5) Ocvirk, G.; Verpoorte, E.; Manz, A.; Grasserbauer, M.; Widmer, H. M. *Anal. Methods Instrum.* **1995**, *2*, 74–82.

(6) Ericson, C.; Holm, J.; Ericson, T.; Hjerten, S. *Anal. Chem.* **2000**, *72*, 81–87.

(7) Seki, M.; Yamada, M.; Ezaki, R.; Aoyama, R.; Hong, J. W. *Proceedings MicroTotal Analysis Systems*, Monterey, CA, October 21−25, 2001; Kluwer Academic Publishers: Dordrecht, The Netherlands, 2001; pp 48−50.

(8) Vahey, P. G.; Smith, S. A.; Costin, C. D.; Xia, Y. N.; Brodsky, A.; Burgess, L. W.; Synovec, R. E. *Anal. Chem.* **2002**, *74*, 177–184.

10.1021/ac802359e CCC: $40.75
Published on Web 03/06/2009

compressed air to separate phenols and vitamins.[9] Following the development of high pressure on-chip valve[10] and injector[11] components by researchers at Sandia National Laboratories using an in situ photopolymerization technique, Reichmuth et al. integrated these components for the development of an HPLC microchip enabling RPLC separations of peptides and proteins.[12] Agilent has more recently developed an HPLC chip technology integrating a sample enrichment column, a packed separation column, and a nanoelectrospray tip for mass spectrometry interfacing,[13] which has been applied to separations of biological samples coupled with mass spectrometry analysis.[14] Other researchers have reported fully integrated pressure-driven HPLC microchips with major components such as pumps, mixers, sample injectors, and separation columns fabricated in a single device.[15−17]

Significant efforts have focused on fabricating efficient chromatographic columns on pressure-driven HPLC microchips. Microfluidic open-tubular columns,[4,8,9] packed-bed columns,[5,7,13,15,16] micromachined pillar array columns,[18] and continuous-bed or monolithic columns[6,12,19] have been reported. While open-tubular columns were the focus of initial chip-based HLPC development due to their low hydraulic resistance, moderate separation performance, and ease of fabrication, they suffer from low sample loading capacity resulting from limited total surface area. While the use of packed-bed columns employing derivatized particles, such as silica beads adopted from capillary separations, can significantly increase the surface area and loading capacity, packing and retaining particles at specific locations within microfluidic devices is nontrivial and can introduce undesirable fabrication and design constraints. As an extension of He and Regnier's early work,[20] Malsche et al.[18] used a deep reactive ion etch (DRIE) process to create a nonporous pillar array within a microchannel and demonstrated fast separation of three coumarin dyes using a pressure-driven RPLC separation. In theory, the ordered pillar microstructure can minimize eddy diffusion and afford higher efficiencies than other HPLC columns,[21] while small loading capacity of the nonporous columns may be overcome by introducing a porous structure on the micromachined pillars.[22] Still, obtaining a uniform coating on the pillar surface remains a major challenge,[21] and the high fabrication costs associated with DRIE limits the viability of this approach for disposable applications.

A particularly effective method to introduce separation media within defined regions of a microfluidic system is to synthesize continuous media beds, or monoliths, by in situ photopolymerization. Monoliths are highly porous inorganic or organic materials originally developed for conventional capillary HPLC separations.[23−27] In comparison to packed columns, monoliths enable fast and efficient separations under relatively low pressures.[28] Monoliths can be readily adapted for different separation mechanisms without further treatments by tuning the prepolymer composition and fabrication process. While thermal polymerization of monoliths has been reported within a polymer microfluidic LC chip integrating a rotary injection valve, separation channel, and on-chip UV detection,[29] photopolymerization-based synthesis offers substantial advantages by enabling the preparation of well-defined monolith geometries within specific regions of complex microchannel networks. This feature has been leveraged for the development of polymethacrylate/acrylate monoliths in microfluidic systems as separation media,[12,30−33] mixers,[34] fluidic controls,[10,35] reactors,[36] and electrospray emitters,[37,38] as well as the demonstration of on-chip solid-phase extraction (SPE).[39,40] However, in the development of microfluidic devices employing photopolymerized monolithic separation media, little work has been reported toward integrated HPLC systems.

Here we report a robust approach to fabricating cyclic olefin polymer (COP) HPLC chips containing in situ photopolymerized polymethacrylate monolithic stationary phases. In addition to achieving HPLC separations of fluorescein-labeled model peptides, protein digest, and intact protein samples using a homogeneous reversed-phase polymethacrylate monolith column, the chips employ an integrated injector/splitter structure allowing the devices to be interfaced with a standard LC pump while maintaining nanoscale flow rates within the separation columns. The in situ photopolymerization process was also employed to fabricate a short monolithic trap column in front of a separation column, enabling online sample cleanup and enrichment prior to HPLC separations of fluorescein-labeled intact proteins.

(9) Schlund, M.; Gilbert, S. E.; Schnydrig, S.; Renaud, P. *Sens. Actuators, B: Chem.* **2007**, *123*, 1133–1141.
(10) Hasselbrink, E. F.; Shepodd, T. J.; Rehm, J. E. *Anal. Chem.* **2002**, *74*, 4913–4918.
(11) Reichmuth, D. S.; Shepodd, T. J.; Kirby, B. J. *Anal. Chem.* **2004**, *76*, 5063–5068.
(12) Reichmuth, D. S.; Shepodd, T. J.; Kirby, B. J. *Anal. Chem.* **2005**, *77*, 2997–3000.
(13) Yin, H. F.; Killeen, K.; Brennen, R.; Sobek, D.; Werlich, M.; van de Goor, T. V. *Anal. Chem.* **2005**, *77*, 527–533.
(14) Yin, H. F.; Killeen, K. *J. Sep. Sci.* **2007**, *30*, 1427–1434.
(15) Xie, J.; Miao, Y.; Shih, J.; Tai, Y.-C.; Lee, T. D. *Anal. Chem.* **2005**, *77*, 6947–6953.
(16) Lazar, I. M.; Trisiripisal, P.; Sarvaiya, H. A. *Anal. Chem.* **2006**, *78*, 5513–5524.
(17) Fuentes, H. V.; Woolley, A. T. *Lab Chip* **2007**, *7*, 1524–1531.
(18) Malsche, W. D.; Eghbali, H.; Clicq, D.; Vangelooven, J.; Gardeniers, H.; Desmet, G. *Anal. Chem.* **2007**, *79*, 5915–5926.
(19) Ishida, A.; Yoshikawa, T.; Natsume, M.; Kamidate, T. *J. Chromatogr., A* **2006**, *1132*, 90–98.
(20) He, B.; Tait, N.; Regnier, F. *Anal. Chem.* **1998**, *70*, 3790–3797.
(21) Eijkel, J. *Lab Chip* **2007**, *7*, 815–817.
(22) De Malsche, W.; Clicq, D.; Verdoold, V.; Gzil, P.; Desmet, G.; Gardeniers, H. *Lab Chip* **2007**, *7*, 1705–1711.
(23) Hjerten, S.; Liao, J. L.; Zhang, R. *J. Chromatogr.* **1989**, *473*, 273–275.
(24) Minakuchi, H.; Nakanishi, K.; Soga, N.; Ishizuka, N.; Tanaka, N. *Anal. Chem.* **1996**, *68*, 3498–3501.
(25) Nakanishi, K.; Soga, N. *J. Non-Cryst. Solids* **1992**, *139*, 1–13.
(26) Nakanishi, K.; Soga, N. *J. Non-Cryst. Solids* **1992**, *139*, 14–24.
(27) Svec, F.; Frechet, J. M. J. *Anal. Chem.* **1992**, *64*, 820–822.
(28) Guiochon, G. *J. Chromatogr., A* **2007**, *1168*, 101–168.
(29) Levkin, P. A.; Eeltink, S.; Stratton, T. R.; Brennen, R.; Robotti, K.; Yin, H.; Killeen, K.; Svec, F.; Frechet, J. M. J. *J. Chromatogr., A* **2008**, *1200*, 55–61.
(30) Le Gac, S.; Carlier, J.; Camart, J. C.; Cren-Olive, C.; Rolando, C. *J. Chromatogr., B* **2004**, *808*, 3–14.
(31) Ro, K. W.; Liu, H.; Knapp, D. R. *J. Chromatogr., A* **2006**, *1111*, 40–47.
(32) Liu, J.; Ro, K. W.; Nayak, R.; Knapp, D. R. *Int. J. Mass Spectrom.* **2007**, *259*, 65–72.
(33) Faure, K.; Bias, M.; Yassine, O.; Delaunay, N.; Cretier, G.; Albert, M.; Rocca, J. L. *Electrophoresis* **2007**, *28*, 1668–1673.
(34) Rohr, T.; Yu, C.; Davey, M. H.; Svec, F.; Frechet, J. M. J. *Electrophoresis* **2001**, *22*, 3959–3967.
(35) Yu, C.; Mutlu, S.; Selvaganapathy, P.; Mastrangelo, C. H.; Svec, F.; Frechett, J. M. J. *Anal. Chem.* **2003**, *75*, 1958–1961.
(36) Peterson, D. S.; Rohr, T.; Svec, F.; Frechet, J. M. J. *Anal. Chem.* **2002**, *74*, 4081–4088.
(37) Koerner, T.; Turck, K.; Brown, L.; Oleschuk, R. D. *Anal. Chem.* **2004**, *76*, 6456–6460.
(38) Bedair, M. F.; Oleschuk, R. D. *Anal. Chem.* **2006**, *78*, 1130–1138.
(39) Yu, C.; Davey, M. H.; Svec, F.; Frechet, J. M. J. *Anal. Chem.* **2001**, *73*, 5088–5096.
(40) Bhattacharyya, A.; Klapperich, C. M. *Anal. Chem.* **2006**, *78*, 788–792.

Existing world-to-chip interfaces also constrain the maximum pressures and solvent flow rates which may be employed in chip-LC systems. The intrinsic large dead volumes in these interfaces can lead to band broadening when off-chip sample loading is required and hinder the formation of well-defined and repeatable on-chip solvent gradients. Additionally, low-pressure interfaces place limitations on achieving homogeneous monoliths within long separation columns. The pressure required to drive mobile phases through long columns may induce leakage or physical damage at these interfaces, constraining further improvements in separation performance of microfluidic HPLC systems. To avoid these issues, a simple high-pressure and low-unswept-volume world-to-chip interface was fabricated using stainless steel needle segments inserted into the COP substrates.[41] Fully integrated devices employing this interface were found to reliably withstand internal pressures above 20 MPa (~2900 psi), sufficient for most HPLC applications, without leakage from the needle interfaces or substrate delamination.

EXPERIMENTAL SECTION

Chemicals. Butyl methacrylate (BMA, 99%), ethylene dimethacrylate (EDMA, 99%), ethylene diacrylate (EDA, 90%), methyl methacrylate (MMA, 99%), 1,4-butanediol (99%), 1-propanol (≥99.5%), cyclohexane (99%), acetonitrile (ACN, reagent grade), 2,2′-dimethoxy-2-phenylacetophenone (DMPA, 99%), benzophenone (BP, 99%), DL-dithiothreitol (DTT, electrophoresis grade), fluorescein isothiocyanate isomer I (FITC, 98%), ribonuclease A, cytochrome C, BSA (96%), neurotensin (98%), bradykinin acetate (98%), [leu^5]-enkephalin (96%), and angiotensin II acetate were purchased from Sigma-Aldrich (St. Louis, MO). Trypsin Gold (mass spectrometry grade) was ordered from Promega (Madison, WI). Methanol, HPLC water, and rhodamine B (RhB, 99+%) were obtained from Fisher Scientific (Pittsburgh, PA). Urea, acetic acid, sodium carbonate, and sodium bicarbonate were ordered from J. T. Baker (Phillipsburg, NJ). Trimethylolpropane trimethacrylate (TMPTMA) was received as a free sample from Sartomer (Warrington, PA).

Microchip Fabrication. The channel network was fabricated using 2.0 mm thick Zeonor 1020R COP substrates (Zeon Chemicals, Louisville, KY) patterned by hot embossing. A silicon template with inverted channel features was first prepared by deep reactive-ion etching (DRIE) (Surface Technology Systems, Newport, U.K.) and then bonded to a stainless steel plate using Pyralux bonding film (DuPont, Wilmington, DE) at 180 °C. The template assembly was clamped on a custom aluminum jig before hot embossing and mounted to the lower platen of a hydraulic press (AutoFour/15; Carver, Wabash, IN), with a 6.4 mm thick glass plate secured on an aluminum holder installed on the upper press platen. A blank COP substrate degassed overnight at 85 °C in a vacuum oven (VWR Scientific, West Chester, PA) was placed between the template and the glass plate, and heated to 128 °C. After applying a pressure of 120 psi (0.83 MPa) for 10 min, the platen temperature was decreased to 95 °C. The COP plate was then released from the press and cooled to room temperature by natural convection.

Schematic diagrams of the HPLC chips are shown in Figure 1. The simple double-T chip depicted in Figure 1A has a 17 cm long serpentine separation channel, which contains a 15 cm long monolithic column for microchip HPLC separations. In addition to the separation channel, the second chip design depicted in Figure 1C includes a 1 cm long channel (dashed line) to accommodate a monolithic trap column, allowing sample cleanup and enrichment to be performed before microchip HPLC separations. For both chip designs, all microchannels possess rectangular cross sections with nominal dimensions of 100 μm width and 60 μm depth.

To seal the microchannel network, the patterned COP substrate was bonded to a COP cover plate predrilled with 650 μm diameter needle access holes using a solvent-bonding process. Before bonding, both the cover and the microchannel plates were degassed overnight in a vacuum oven at 85 °C. The cover plate was used to seal a glass container partially filled with cyclohexane, with the bonding side of the cover plate positioned 5 cm from liquid solvent surface. The container was heated to 30 °C to generate a controlled cyclohexane vapor pressure to solubilize the exposed COP surface. After 8.5 min, the cover plate was removed from the container and manually aligned and pressed to the hot embossed substrate. The chip assembly was immediately placed in the hydraulic press at 300 psi (2.07 MPa) for 10 min at room temperature to achieve a permanent bond.

Needle Interface Fabrication. To form high-pressure interfaces to off-chip capillaries required for the HPLC separations, 2.54 cm long segments of 22 gauge surgical needle (710 μm o.d., 400 μm i.d., Hamilton, Reno, NV) possessing flat polished ends were thoroughly cleaned with methanol and water and then dried with nitrogen gas. Each needle segment was tightened in a keyless drill chuck (Albrecht, Hauppauge, NY) installed on a bench press and carefully inserted to the bottoms of the 650 μm wide access holes with the help of an inspection stereomicroscope. Immediately after interface fabrication, the HPLC chip was annealed in a vacuum oven at 85 °C for 4 h to release stress generated during needle insertion.

In Situ Fabrication of Monolithic Stationary Phase. The surface of the COP channel network was functionalized using a photografting method[42] to provide an anchoring layer for the monolithic stationary phase. Briefly, the COP channel network was thoroughly rinsed with methanol, dried in the vacuum oven at room temperature, and filled with a reaction solution containing 49.5 wt % EDA, 49.5 wt % MMA, and 1.0 wt % BP, which has been sonicated for 30 min. The device was then exposed to a UV source (PRX-1000; Tamarack Scientific, Corona, CA) with a power of 24.0 mW/cm^2 for 630 s. Followed UV photografting, the channel network was again rinsed with methanol and dried in the vacuum oven. The reversed-phase monolithic stationary phase was synthesized by in situ photopolymerization. First, a reaction solution containing 24.5 wt % BMA, 14.5 wt % TMPTMA, 30.0 wt % 1-propanol, 30.0 wt % 1,4-butanediol, and 1.0 wt % DMPA was degassed for 30 min by sonication and injected into the treated COP microchannel network. After a 480 s UV exposure using a photomask to define the photopolymerization region, a 15 cm long RP monolith was formed within the serpentine

(41) Chen, C. F.; Liu, J.; Hromada, L.; Tsao, C. W.; Chang, C. C.; DeVoe, D. L. *Lab Chip* **2008**, *9*, 50–55.

(42) Stachowiak, T. B.; Rohr, T.; Hilder, E. F.; Peterson, D. S.; Yi, M. Q.; Svec, F.; Frechet, J. M. J. *Electrophoresis* **2003**, *24*, 3689–3693.

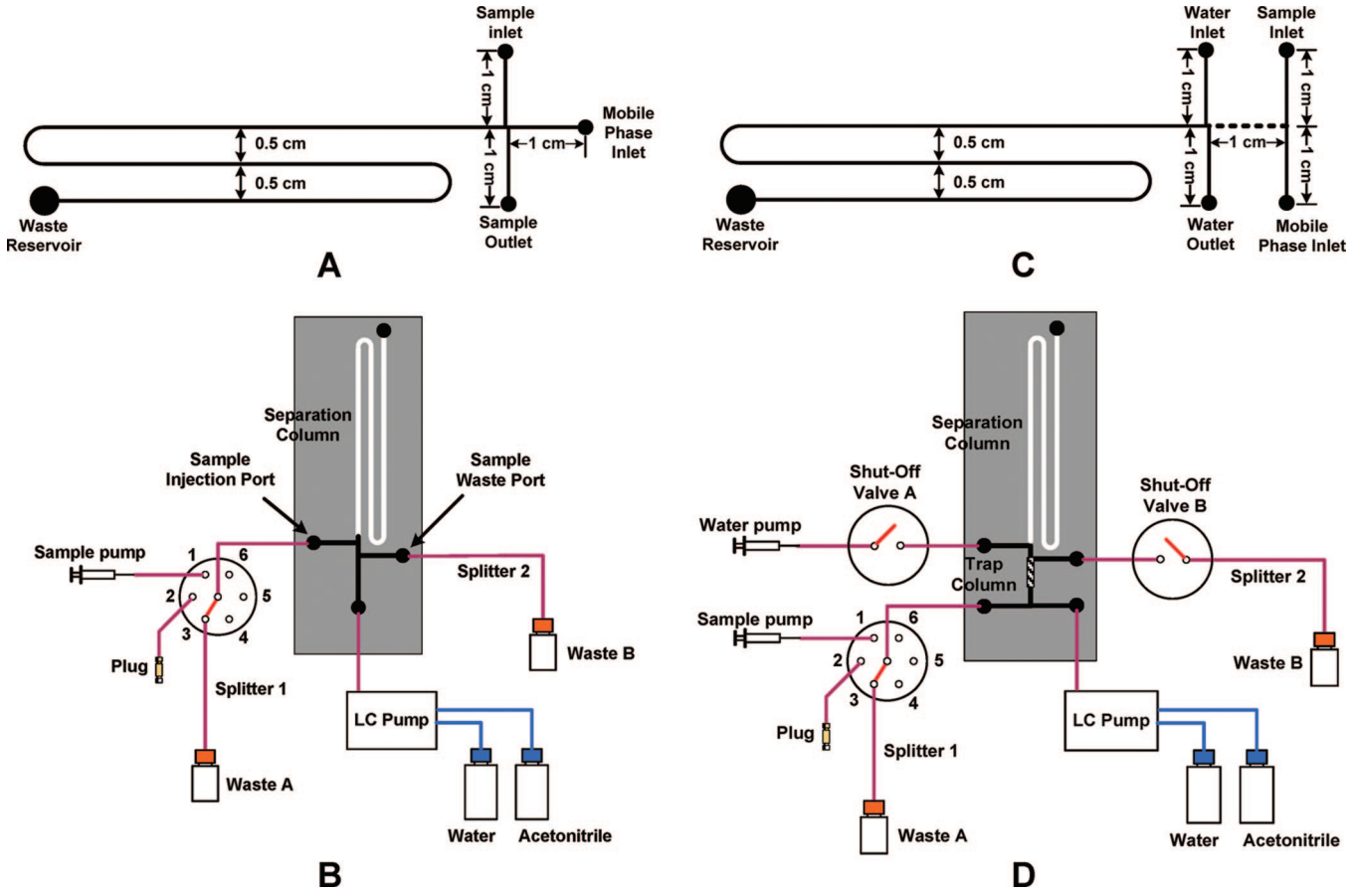

Figure 1. (A) Chip design and (B) experimental system for HPLC separations employing dynamic sample injection, (C) chip design and (D) experimental system for online sample cleanup/enrichment-HPLC separations, with an integrated 5 mm long SPE trap column used for online sample cleanup and enrichment. The total length of the serpentine separation channels is 17 cm in both chip designs.

separation channel, with its end 2 cm away from the waste reservoir (Figure 1A). The same procedures were followed to prepare a 5 mm long trap column and a 15 cm long separation column in the device shown in Figure 1C. During photopolymerization, the trap column was positioned in the channel depicted by the dashed line (Figure 1C) and the separation column prepared in the serpentine channel with a photomask.The resulting monolith was rinsed with methanol at 1 μL/min for 12 h before use.

Preparation of BSA tryptic digest. BSA was dissolved in a solution containing 8 M urea, 5 mM DTT, and 10 mM sodium carbonate/bicarbonate buffer (pH 9.3) to a concentration of 5 mg/mL. The solution was incubated at 95 °C for 20 min and then cooled to room temperature. The denatured BSA was diluted 2-fold with 10 mM sodium carbonate/bicarbonate buffer. Trypsin was reconstituted with a 50 mM acetic acid solution and added to the diluted denatured BSA solution according to a weight ratio of 1:50 (trypsin/BSA). Digestion was allowed to proceed at 37 °C for 20 h.

Preparation of FITC-Labeled Peptide and Protein Samples. Each model peptide was dissolved in 10 mM sodium carbonate/bicarbonate buffer (pH 9.3) to a concentration of 2 mM, and then 200 μL of each 2 mM peptide solution was mixed with 50 μL of 6 mM FITC acetone solution. FITC-labeled BSA tryptic digest was prepared by mixing 150 μL of 6 mM FITC acetone solution with 600 μL of BSA tryptic digest solution. The labeling reaction was allowed to proceed in the dark for 24 h.

The model peptide sample was prepared by mixing an equal volume of labeled peptide solutions and then diluting 5 times with HPLC water. The FITC-labeled BSA tryptic digest sample was diluted 3-fold with HPLC water before being injected to the HPLC microchip at a final concentration of 0.6 mg/mL.

FITC-labeled proteins were prepared by dissolving each model protein to 100 mM sodium carbonate/bicarbonate buffer (pH 9.3) to a concentration of 100 μM and mixing the solution with 20 mM FITC acetone solution. The molar ratio of FITC to the protein was adjusted to 10:1 in the solution. The reaction vessel was placed in the dark undisturbed for 24 h, and the product was diluted 20−400 times with HPLC water before use.

Microchip HPLC and Online Sample Cleanup/Enrichment-HPLC Separations. Microchip HPLC separations without on-chip sample cleanup and concentration were performed using the instrument setup shown in Figure 1B. Silica capillary sections (360 μm o.d. and 100 μm i.d., Polymicro, Phoenix, AZ) were used to connect the microchip to external pumps and valves. A 50 cm long capillary section was connected to the sample waste port as a splitter. The 50 cm long capillary section extending from position 3 of the 6-way microselection valve (Upchurch) to waste A served as a second splitter during separation. The dwell volume of the final setup was estimated to be 800 μL. During sample injection, the selection valve was set at position 1, and sample was injected into the microchip at a flow rate of 4 μL/min using a PHD-2000 syringe pump (Harvard Apparatus, Holliston, MA). Water was

simultaneously pumped to the microchip at a flow rate of 20 μL/min using a PU-2089 analytical LC pump (Jasco, Easton, MD) to force a portion of the sample stream to enter the separation channel. After injecting the desired quantity of sample, the syringe pump was stopped, the selection valve was quickly set to waste A at position 3, and a linear ACN gradient from the LC pump was initiated to elute and separate the analytes stacked at the head of the monolith column. The master flow rate was set between 1−2 mL/min (1% RSD). The flow rate within the separation column was estimated by measuring the time required to fill the 5 μL end reservoir loosely covered with a small piece of blue dicing tape (Semiconductor Equipment, Moorpark, CA), which was found to be within 200−500 nL/min (2% RSD) depending on the mobile phase, resulting in solvent splitter ratios ranging from 2000:1 to 5000:1 for the given splitter geometry.

When combining online sample cleanup/enrichment prior to HPLC separations, the apparatus depicted in Figure 1D was employed. Following sample injection, the selection valve was switched to position 1 and shut-off valves A and B were opened. Sample was loaded onto the polymethacrylate monolith trap column at a flow rate of 4 μL/min using a syringe pump (sample pump) while simultaneously pumping water from the LC pump at a flow rate of 4 μL/min. The water flow from the LC pump during sample loading was used to ensure that all injected sample was directed onto the trap column. A second syringe pump (water pump) was used to deliver water at a flow rate of 2 μL/min through shut-off valve A to the microchip, which served to prevent the sample stream entering the separation column. Immediately after injecting sample for a set period of time to achieve the desired loading amount, the sample pump was turned off and the selection valve switched to position 2 to stop the injection, while the LC pump and the water pump were kept on for 5 min to rinse the sample adsorbed on the trap column with water. Followed this rinsing step, the water pump was stopped, the selection valve was switched to position 3, both shut-off valves were turned off, and a linear ACN gradient was delivered to the microchip using the LC pump to elute the cleaned/enriched sample off the trap column to the separation column for HPLC separation. The master flow rate was set at 0.7 mL/min (1% RSD), and the flow rate in the separation column was estimated to be 200 nL/min (3% RSD), resulting in a split ratio of 3500:1.

Before each sample injection, at least three blank runs using the same ACN gradient as in the separations were performed to condition the reversed-phase monolithic columns and remove residual sample from previous separations, which helped to improve separation reproducibility and prevent sample carryover.

Data Collection. The HPLC chip was positioned on the stage of a TE-2000 S inverted epi-fluorescence microscope (Nikon, Melville, NY) for detection and the detection point was positioned immediately after the end of the separation column. An excitation wavelength within the range of 465−495 nm was selected using a B-2E/C blue filter (Nikon) to detect the separated FITC-labeled peptides. A 4×, 0.20 N.A. objective (Nikon) was used for simultaneous imaging and detection. Images and videos were recorded using a CoolSnap HQ2 CCD camera (Roper Scientific, Tucson, AZ) installed on the microscope. Chromatograms were obtained using Nikon Elements image analysis software.

RESULTS AND DISCUSSION

Microchip Fabrication. Longer separation columns are generally desirable to provide higher peak capacities and theoretical plate numbers for chromatography separations. However, monolithic columns in most previously reported polymer HPLC microchips are typically only several centimeters long, a constraint which presumably results from the high pressures needed to drive the mobile phase through longer columns exceeding the pressure limits of the chips. While the commonly used thermal bonding method can provide only moderate bonding strength,[43] solvent bonding offers much stronger bonds,[44] since solvated polymer chains at the bonding surfaces can interpenetrate each other more effectively. Solvent bonding can be performed at temperatures well below the glass transition temperature of the polymer substrates, allowing channel deformation to be minimized or eliminated. To avoid dissolving the COP microchannels by excess solvent, degassed COP plates were exposed to gas-phase solvent in an enclosed chamber filled with cyclohexane vapor, as opposed to directly applying liquid-phase solvent to the substrate surfaces. Unlike previous approaches,[31,45] the microchips were held at room temperature for an extended period after bonding, followed by an annealing process for stress relief. In both pressure testing and HPLC separations, these treatments were found to be essential for achieving reliable high-pressure bonding with no delamination.

The COP HPLC chips reported here employ a simple, low cost, and adhesive-free world-to-chip interface consisting of 22 gauge stainless steel surgical needle sections (~710 μm o.d. and ~400 μm i.d.), which can be directly interfaced to external pumps, valves, or other devices through standard capillary connectors. When a needle is inserted into a milled hole within the COP substrate with a diameter of 650 μm, deformation of the polymer matrix generates residual compressive stress resulting in high frictional force between the COP substrate and sidewall of the inserted needle. By positioning the blunt needle tips at the bottom of the cover plate access holes, which are centered above the microchannels in the lower COP plate, dead volume introduced by the interface is effectively eliminated. Following initial needle insertion, 150−250 μm long cracks were often observed surrounding the needle periphery following 24 h storage at room temperature. However, after subjecting the chips to an annealing process to reduce residual stress around the hole, very few cracks were observed. By gradually increasing water flow rate in test chips containing 3.3 cm long monoliths, delamination was observed at an average pressure of 23.8 MPa (3451 psi), while physical ejection of the needles from the milled holes required an average pressure of 40 MPa (5800 psi),[41] far exceeding the typical bond strength of the COP substrates.

Monolith Preparation. When using a previously reported BMA-EDMA recipe for monolith preparation,[46] the stationary phase along the 15 cm length of the separation channel was found to be discontinuous, with a uniform monolith observed only within the central section, approximately 5 cm long, while the majority of the channel contained discrete porous clusters with lengths

(43) Tsao, C. W.; Hromada, L.; Liu, J.; Kumar, P.; DeVoe, D. L. *Lab Chip* **2007**, *7*, 499–505.
(44) Kelly, R. T.; Pan, T.; Woolley, A. T. *Anal. Chem.* **2005**, *77*, 3536–3541.
(45) Mair, D. A.; Rolandi, M.; Snauko, M.; Noroski, R.; Svec, F.; Frechet, J. M. J. *Anal. Chem.* **2007**, *79*, 5097–5102.
(46) Geiser, L.; Eeltink, S.; Svec, F.; Frechet, J. M. J. *J. Chromatogr., A* **2007**, *1140*, 140–146.

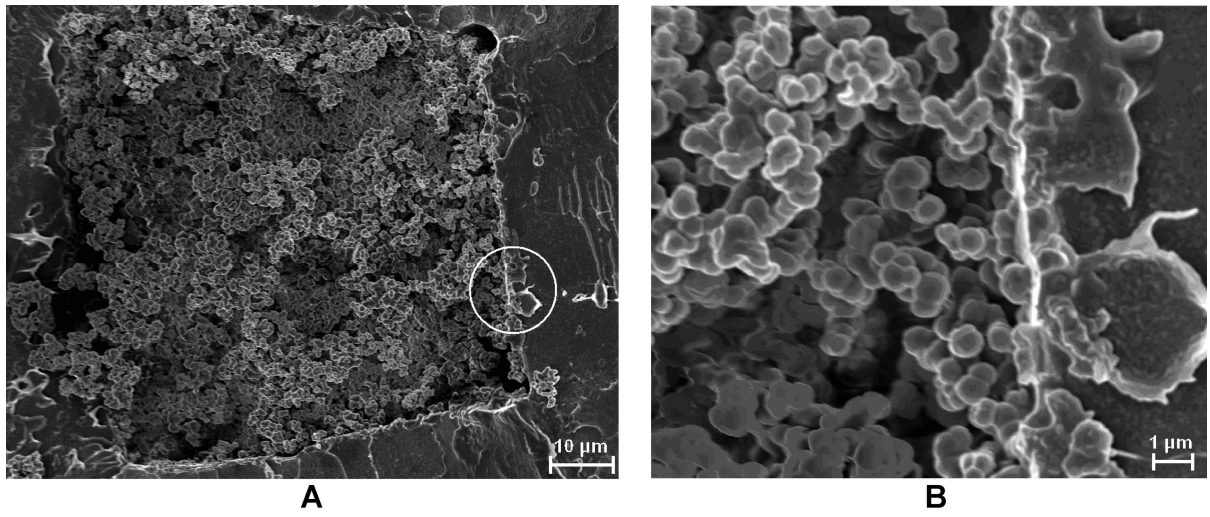

Figure 2. (A) SEM images of BMA-TMPTMA monolith. (B) Magnification of the circular area in part A revealing apparent covalent attachment of monolith to the COP channel surface.

ranging from ~100 to 1000 μm. This phenomenon has also been observed by Ramsey and Collins,[47] and is believed to be caused by localized fluid flow during in situ photopolymerization. To eliminate this problem, access holes were sealed and chips were left undisturbed for at least 10 min before photopolymerization to minimize pressure gradients within the channels. Although the overall continuity of the monolith was improved to some degree using this approach, discrete clusters were still observed along the separation channel. Similar results were observed when modifying other factors such as UV exposure time and photoinitiator concentration. Alternative porogens, namely, 1-decanol and cyclohexanol,[48] were also evaluated. However, the resulting BMA-EDMA monoliths either still exhibited discrete clusters or showed extremely low permeability to the mobile phase.

To produce a suitable morphology for the RP monoliths, TMPTMA was explored as an alternative to EDMA as a cross-linker for monolith formation. When EDMA was replaced with TMPTMA, the resulting BMA-TMPTMA monolith exhibited a continuous structure along the entire length of the separation channel using the same preparation conditions. This striking improvement in monolith structure presumably results from TMPTMA, a multifunctional monomer with three methacrylate groups, which dramatically increases the density of reaction centers in the solution, providing additional seeds for the formation of a more homogeneous monolith. It was also possible that during the polymerization, the rapidly grown bulk BMA-TMPTMA polymers at the active reaction centers suppressed the free diffusion of monomers or oligomers over long distances to previously activated centers, thus forcing local polymerization around the reaction center to form a fine network in both the axial and radial directions.

Grafnetter et al. characterized the hydrophobicity of BMA-EDMA monolithic stationary phases recently and found the Walters hydrophobicity indexes (HI) of the phases are within the range of 3.6~4.3.[49] The composition of the main hydrophobicity provider BMA in the BMA-TMPTMA monolith is similar to that of the BMA-EDMA monoliths. Only the cross-linkers are different. Therefore, the HI value or hydrophobicity of the BMA-TMPTMA monolith is expected to be close to that of the BMA-EDMA monoliths. In comparison, the HI values of typical Zorbax SB-C_{18} and Rx-C_{18} octadecylsilane (ODS) modified silica phases are 4.26 and 4.84, respectively,[50] suggesting that the hydrophobicity of BMA monolithic phases is lower but still comparable to that of conventional ODS reversed phases.

An SEM image of a monolith fabricated using the modified BMA-TMPTMA recipe is shown in Figure 2A, revealing the porous structure typical of a BMA-containing RP polymethacrylate monolith. The monolith morphology consists of numerous clusters of fused globules with diameters smaller than 1 μm, while the globular clusters agglomerate to form many large irregular through-pores. The magnified view of the SEM image in Figure 2B also reveals that the monolith is anchored to the COP channel surface, presumably through covalent bonds, to prevent bulk movement of the monolith under high pressure and the formation of an interfacial gap between the channel wall and monolith, which would lead to sample leakage during separation. It should be mentioned that SEM images cannot provide direct evidence of covalent bond formation. To reveal the true nature of the attachment, it is necessary to employ special surface analysis methods such as X-ray photoelectron spectroscopy and attenuated total reflection-Fourier transform infrared spectroscopy.

On-Chip Sample Injection. Off-chip injection of sample into microfluidic separation columns with monolithic stationary phases has been reported by hyphenating pumps, flow splitters, and injection valves to LC chips through a variety of world-to-chip interfaces.[6,30−32] An important consideration when using off-chip sample injection valves is the potential for band broadening and dilution of the injected sample volume due to dead volumes introduced by the chip interface and the connecting capillaries/channels. Use of on-chip injection can eliminate this issue by integrating the injector adjacent to the separation column.

Reported approaches to on-chip sample injection for pressure-driven HPLC chips include microvalve injectors,[12] channel junction

(47) Ramsey, J. D.; Collins, G. E. *Anal. Chem.* **2005**, *77*, 6664–6670.
(48) Lee, D.; Svec, F.; Frechet, J. M. J. *J. Chromatogr., A* **2004**, *1051*, 53–60.
(49) Grafnetter, J.; Coufal, P.; Tesařová, E.; Suchánková, J.; Bosáková, Z.; Ševčík, J. *J. Chromatogr., A* **2004**, *1049*, 43–49.
(50) Scholten, A. B.; Claessens, H. A.; de Haan, J. W.; Cramers, C. A. *J. Chromatogr., A* **1999**, *759*, 37–46.

injectors,[17−19] on-chip injection loops,[29] and trap columns.[13,15,16] Reproducible sample injection has been achieved with adjustable sample loading using integrated microvalve injectors, but implementation of this approach requires high-pressure polymer pistons which complicate device fabrication and system operation. Channel junction injectors, such as the common double-T configuration,[51] provide a simple approach to meter short sample plugs defined by the geometry of the channel junction, but only fixed injection volumes are possible using this scheme. While gated electrokinetic injection through on-chip channel junctions enables sequential injection of multiple sample volumes, it can introduce electrokinetic injection bias while also increasing system complexity. The on-chip injection loop is a recent development of the chip-based injection scheme by Agilent Technologies, which provides high reproducibility in sample loading. Unfortunately, similar to the channel junction injector, the sample loading amount is limited by the volume of the loop. Although induced injection bias can be reduced by selectively adsorbing analytes to the stationary phases, trap columns are still an attractive injection method for on-chip separations since they offer relatively large loading capacity and can be used as SPE columns prior to chromatographic separations for sample cleanup and enrichment, two important processes in many analytical applications for reducing the impact of matrix effects of complex real-world samples and improving detection sensitivity. Yin et al.,[13] Xie et al.,[15] and Lazar et al.[16] employed a short on-chip C18 trap column for sample enrichment before RPLC separation. Dahlin et al. integrated a reversed phase polystyrene SPE column in a PDMS capillary electrophoresis microchip for desalting and sample enrichment.[52] Ramsey and Collins demonstrated over 200 times preconcentration of fluorescent dyes prior to on-chip micellar electrokinetic chromatography using a C18 SPE column.[47] In each of these examples, spherical polymer or silica particles were packed into microfluidic channels to form the porous SPE beds. While this packing approach can be convenient for simple channel designs, it becomes increasingly difficult to form columns at specific positions in microfluidic devices with more complex channel networks, such as the present chip design where isolated SPE and separation columns are desired. In this case, a more effective solution is to synthesize monolithic phases using in situ photopolymerization. Two on-chip injection schemes are described here, namely, pressure-controlled dynamic sample injection and in situ fabricated monolithic trap column injection.

Dynamic sample injection was employed in HPLC chips with simple double-T channel junction injectors to enable variable sample loading amounts. As shown in Figure 3A, a sample flow from a to b was initially established and water was simultaneously delivered from c to b to divert a portion of the sample to the separation channel. After injecting the desired amount of sample, the flow path was changed using the off-chip selection valve in Figure 1B and an ACN gradient was introduced from c to elute and separate the analytes stacked at the head of the RP monolithic column. In this process, the double-T channels served as a connector to the splitters to shunt a defined portion of mobile phase to wastes (c to a and c to b), thus maintaining the flow rate

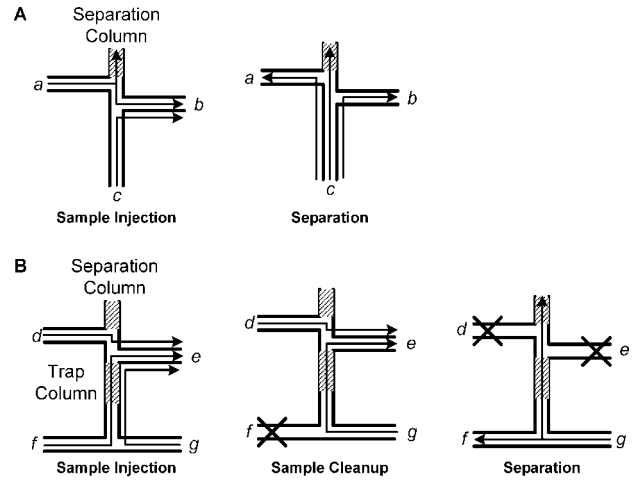

Figure 3. Details of chip operation: (A) HPLC separation using dynamic sample injection and (B) online sample cleanup/enrichment-HPLC separation.

in the separation channel at the desired nanoflow level, and flushing residual sample in the side channel to waste to eliminate sample carryover.

To fabricate the HPLC chips employing trap columns, a 5 mm long monolithic trap column was fabricated within the 1 cm long channel section depicted as a dashed line in Figure 1C. Both columns were synthesized from the same BMA-TMPTMA prepolymer. In a typical injection using the monolithic trap column (Figure 3B), water streams from d to e and from g to e are used to direct sample flow (f to e) onto the SPE trap column. As sample was passed through the hydrophobic trap column, the dilute analytes were retained and enriched on the column, along with a portion of matrix components. To purify the bound analytes, sample delivery (f to e) was stopped using the off-chip selection valve (Figure 1D) while the two water flows (d to e and g to e) were maintained until weakly retained matrix species such as unlabeled dyes, chaotropic reagents, or high concentration salts were flushed to the waste reservoir. Following sample cleanup, the water flow from d to e was stopped by closing the shut-off valves (Figure 1D). Meanwhile, the selection valve was switched to connect the splitter to f, and an ACN gradient was delivered to g to start the gradient separation. In the sample cleanup process, the off-chip valve connected to the sample inlet channel f (Figure 3B) was closed, A negligible amount of sample was found to leak to the trap column at the beginning of the process due to the pressure pulse generated by valve closing. The sample residue trapped in f did not enter the trap column throughout sample cleanup and was completely flushed out during LC separation. During the separation, the enriched analyte bands protruded 200∼300 μm into the side arms d and e (Figure 3B) when passing these sections, resulting in sample loss and band broadening. Furthermore, residual sample remaining in the side arms can potentially leak to column, causing undesired sample carryover. These problems are introduced by the dead volumes intrinsic to the off-chip shut-off valves and the connectors, which can be eliminated by using on-chip valves with true zero dead volumes.

In the trap column injection method, the pH and ionic strength of the background buffer could be independently adjusted during each stage of the process for optimal analyte retention and separation efficiency by isolating the flow paths for SPE sample

(51) Jacobson, S. C.; Hergenroder, R.; Koutny, L. B.; Ramsey, J. M. *Anal. Chem.* **1994**, *66*, 2369–2373.
(52) Dahlin, A. P.; Bergstrom, S. K.; Andren, P. E.; Markides, K. E.; Bergquist, J. *Anal. Chem.* **2005**, *77*, 5356–5363.

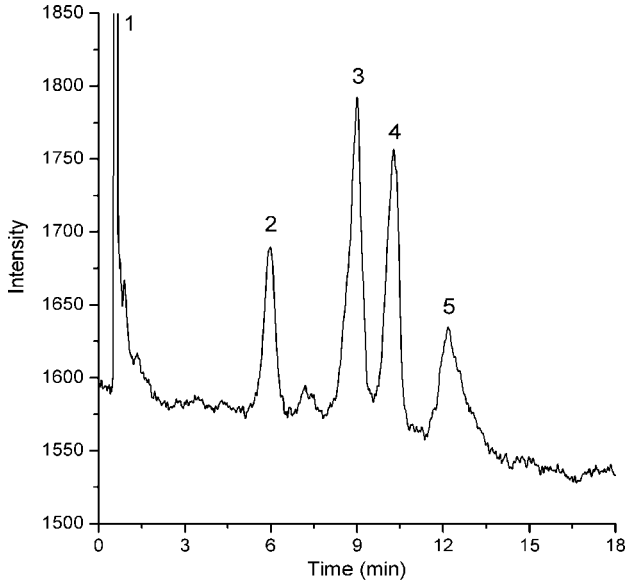

Figure 4. Separation of a mixture of four FITC labeled model peptides. Peak elution order is (1) FITC, (2) angiotensin II, (3) [leu^5]-enkephalin, (4) neurotensin, and (5) bradykinin. A 15 min linear ACN gradient from 5% to 20% was employed during separation, with a master flow rate of 2 mL/min and a column flow rate of 500 nL/min. Injection time was 40 s for an estimated total loading of 11 ng.

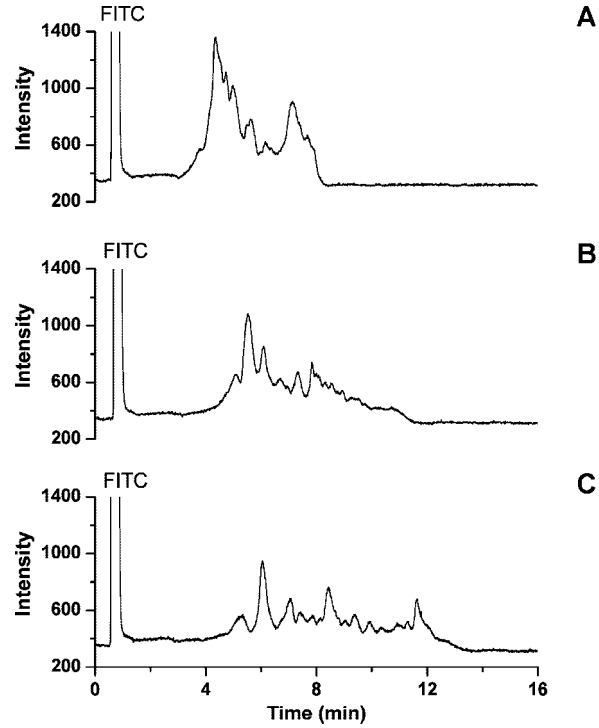

Figure 5. HPLC separation of FITC labeled BSA tryptic digest using different linear ACN gradients: (A) 8%, (B) 5%, and (C) 3.5% ACN/min. Injection time was 1 min, master flow rate was 1 mL/min, and column flow rate was 200 nL/min. With the use of the three labeled peptide peaks, an average retention time variance of 2.9% was determined for the 10 min gradient case.

loading and separation column injection. Although not examined here, it is also possible to subject the adsorbed analytes to multiple chemical reactions without affecting the subsequent separations by exploiting the isolated flow scheme, which further expands the range of potential applications of the microdevices.

HPLC Separation of FITC Labeled Peptides Using Dynamic Sample Injection. A mixture containing four FITC-labeled model peptides (0.1 mg/mL for each peptide) was introduced into the HPLC chip using dynamic sample injection. The peptide sample entered the separation channel (width, 100 μm; depth, 60 μm) at a measured linear velocity of 120 μm/s during the 40 s injection, resulting in a total loading amount of 11 ng. Because FITC exhibits low fluorescence under acidic conditions, the mobile phase was maintained at neutral rather than acidic pH as commonly practiced for peptide separations. At pH 7, unlabeled FITC dye was weakly retained by the BMA-TMPTMA monolith and eluted off the column rapidly at the beginning of the ACN gradient.

As shown in Figure 4, complete separation of the peptides was achieved using a solvent gradient from 5% to 20% at a rate of 1% ACN/min. Relative standard deviation (RSD%) values of peptide retention time ($n = 3$) were 1.1%, 3.4%, 3.4%, and 3.7% for peaks 2, 3, 4, and 5, respectively. Peak height RSD% was less than 8%.

LC pump flow rate variance is one potential source of the observed retention time variance. Additionally, variations may arise from irreproducible monolith swelling in the solvent gradient with monotonically increasing ACN concentration, resulting in unpredictable changes in permeability and monolith surface morphology, and thus variations in both flow rate and peptide retention. In addition to using a high-precision nanoflow LC pump, monoliths with higher rigidity can be employed to reduce the retention time variance. Increasing the amount of cross-linker or using monomers that can form strong polymer networks (e.g., styrene and its derivatives) are effective methods to prepare rigid polymer monoliths. Because of their immunity to the swelling effect of organic solvents and excellent separation performances, inorganic monolithic stationary phases such as silica monolith should also be considered as a viable alternative.

It was found that the peak heights of all samples varied together, and the variations of the normalized peak height based on the free dye peak approached zero. Therefore, the relatively high peak height variance is believed to result from pressure pulses generated during sample injection. As the selection valve was switched from position 3 to 1 to connect the syringe pump to the on-chip injector (Figure 1A), residual pressure from the previous run was suddenly released, resulting in an unpredictable fluctuation in sample flow and hence a variation in sample loading. This injection irreproducibility is inherent to the dynamic injection scheme.

Separation of a more complex peptide sample, FITC-labeled BSA tryptic digest, was also evaluated. Figure 5 shows the separation of the digest with different linear ACN gradients, with the best separation performance realized using a shallow gradient of 3.5% ACN/min. Using the three major peaks 1, 2, and 3 in Figure 5C to evaluate retention time variance, the separations were found to be repeatable, with an average RSD % value ($n = 5$) of 2.9%. The use of longer elution times with shallower solvent gradients below 3.5% ACN/min further improved separation resolution, but with a corresponding reduction in peak height which prevented effective detection of low-intensity peaks.

Liu et al. recently demonstrated on-chip RPLC-MS analysis of BSA tryptic digest using a UV-polymerized polymethacrylate [poly(ethylhexyl methacrylate-*co*-ethylene glycol dimethacrylate), PEHMA-EDMA] monolith,[32] with the resulting total ion chro-

matogram revealing many small peaks grouped into several large well-resolved clusters. In contrast, in the present work all major detectable BSA digest peaks were evenly distributed in a separation window between 5 and 12 min (Figure 5C), with no additional peaks appearing after 14 min. This is likely caused by fundamental differences in both morphology, hydrophobicity, and physical properties such as porosity between the PEHMA-EDMA and BMA-TMPTMA monoliths, together with differences in separation conditions, e.g., mobile phase pH values, flow rates, and solvent gradients. Furthermore, unlabeled or poorly labeled peptides are not represented in the chromatogram presented in Figure 5.

Finally, it is notable that more than 100 LC runs including 40 peptide separations were performed using a single HPLC chip over a 1 month period with no monolith damage, leakage, or substrate delamination observed, reinforcing the reliability and robustness of the fabrication techniques presented here. It should also be emphasized that dynamic sample injection exploits injection volumes defined by simple channel geometry to implement regular chip LC separations. Qualitative separation results can be obtained with this method. However, as revealed in the peptide separation experiments, dynamic injection has intrinsic issues including relatively large sample consumption, small sample loading, and difficult injection control, implying a more robust injection method that can overcome these problems is needed.

Online Sample Cleanup/Enrichment-HPLC Separation. To demonstrate online sample cleanup/enrichment-HPLC separation, a simple protein mixture containing 0.25 μM FITC-labeled ribonuclease A and 0.5 μM cytochrome C was loaded to the trap column at a flow rate of 4 μL/min for 1.5 min, corresponding to a total loading amount of 57 ng. As a control, the same proteins with 10-fold higher concentrations were injected to an HPLC chip using dynamic sample injection under the same conditions as those used for peptide separations. The loading time was 1.5 min and the protein loading was estimated to be 6 ng. Figure 6A shows a HPLC microchip separation of a protein mixture injected using dynamic sample injection, while Figure 6B depicts a HPLC separation of the same protein sample after sample cleanup/enrichment processes. The separation conditions were the same in parts A and B of Figure 6. Peaks 1a and 1b on both chromatograms possibly originated from ribonuclease A labeled with different numbers of FITC, while peak 2 is assigned to FITC-cytochrome C. The two small peaks appearing at 10.5 and 11 min in Figure 6B did not appear in every separation. It is possible when the eluted enriched sample passed sidearms d and e of the chip (Figure 3B), a small amount was trapped. As the separation proceeded, LC pump pressure surge caused the trapped sample to leak to the separation column, resulting in the appearance of these "ghost peaks". The free FITC can be found in the chromatograms of microchip HPLC as the first peak (Figure 6A). When the trap column was used to cleanup the sample, however, the dye was effectively removed and did not appear in the resulting chromatogram (Figure 6B). Because of the high concentration of unbound FITC within the separation column for the dynamic injection case, the peak height of the free FITC is greater than those of the other species and often saturated the CCD detector, preventing the detection of any peaks which may coelute with the unbound FITC dye. The trap column injection and dynamic sample injection methods can both concentrate the sample before

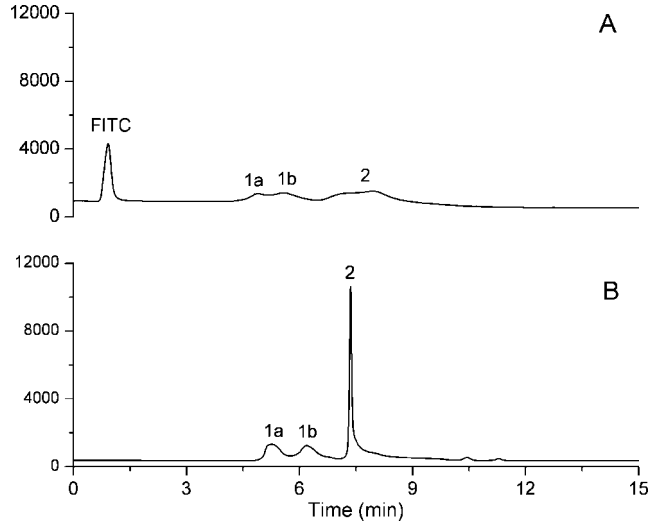

Figure 6. HPLC separation of FITC labeled ribonuclease A (1a, 1b) and cytochrome C (2) using (A) dynamic sample injection and (B) online sample cleanup/enrichment prior to HPLC separation. All separations employed a 4 min linear ACN gradient from 20% to 85%, injection time of 1.5 min, master flow rate of 700 μL/min, and estimated column flow rate of 200 nL/min. The sample in part A contained 2.5 μM ribonuclease A and 5.0 μM cytochrome C. The protein concentration of the sample used in part B was 10 times lower due to the efficiency of sample concentration using the SPE trap column.

separation. However, as expected, the trap column injection approach showed higher sample enrichment efficiency. Estimating from the chromatograms in Figure 6, we found that FITC-ribonuclease A peaks were about 2 times higher while FITC-cytochrome C peak was 15 times higher in the separation using trap column injection. Although the protein sample injected to the trap column had a total concentration 10 times lower than that of the sample loaded directly to the head of the separation column with dynamic sample injection, it was estimated that ~57 ng of proteins was loaded onto the separation column with trap column injection, while only 6 ng was loaded using dynamic sample injection. It should be mentioned that the peak height improvement of FITC-cytochrome C was much greater than that of FITC-ribonuclease A, which could be caused by the fact that the BMA-TMPTMA trap column tended to adsorb more analytes with higher hydrophobicity. The use of the integrated trap column also impacted separation performance. When the on-chip trap column was introduced in the microchip HPLC separation, the resolution of peaks 1a and 1b was improved from 0.6 to 1.2, while the peak width decreased by 40% for peak 1a and 50% for peak 1b (Figure 6). Most striking was that the peak width of FITC-cytochrome C decreased at least 10-fold. Similar performance improvements resulting from incorporation of a trap column into the separation system were reported by Huber's group,[53] who noted that the improvement was mainly due to peak focusing in the trap column. During sample cleanup process in our experiment (Figure 3B), the trapped proteins were rinsed with two water streams (g to e and d to e), which helped to pinch the sample to a narrow plug and thus reduce extra-column band broadening.

(53) Schley, C.; Swart, R.; Huber, C. G. *J. Chromatogr., A* **2006**, *1136*, 210–220.

CONCLUSIONS

Pressure-driven COP HPLC microchips employing in situ photopolymerized polymethacrylate monoliths have been demonstrated using a simple and robust fabrication approach. The chips were bonded using a cyclohexane solvent vapor process and employed high-pressure world-to-chip interfaces with low dead volumes fabricated by inserting surgical needle sections to the access holes of the COP chips. The finished microdevices were able to reliably withstand back pressures well above 20 MPa (~2 900 psi) without interface leakage or substrate delamination. On-chip dynamic sample injection and passive solvent splitting were performed in the same double-T channel junction, allowing the use of a conventional LC pump for microfluidic HPLC separations. Using the microchip HPLC system, gradient separation of FITC-labeled model peptides and BSA tryptic digest were demonstrated on the 15 cm long BMA-TMPTMA RP monolith patterned in the separation channel. A 5 mm long BMA-TMPTMA monolithic trap column was photopolymerized ahead of the separation channel, allowing sample cleanup/enrichment and gradient LC separation to be performed within the same microchip. Also found in the protein separation was that the trap column helped to reduce the injected sample volume and improve the separation performance.

The microchip HPLC system provides a foundation for further developments in pressure-driven microanalysis devices, which can benefit from on-chip dynamic sample injectors, flow splitters, and photolithographically defined polymethacrylate monoliths for high-throughput biomolecular analysis. Incorporation of a monolithic trap column in the HPLC microchip endows the device with capabilities beyond mere separation. With the integration of more functional modules such as dialysis membranes, microfilters, microreactors, microvalves, and monolithic phases with different selectivities, complex sample handling processes and multidimensional separations can be performed on a single microdevice to directly analyze real biological samples.

ACKNOWLEDGMENT

This research was supported by the National Institutes of Health (Grant R01 GM072512) and the National Science Council, Taiwan (Grant NSC 96-2811-E-002-054).

Received for review November 7, 2008. Accepted February 16, 2009.

AC802359E